

Bootstrap current calculations with the SPBSC and the VENUS+ δf codes for the Large Helical Device

M. Yu. Isaev, K. Y. Watanabe¹, W. A. Cooper², M. Yokoyama¹,
H. Yamada¹, O. Sauter², T. M. Tran², A. Bergmann³,
C. D. Beidler⁴ and H. Maaßberg⁴

Nuclear Fusion Institute, RRC “Kurchatov Institute”, Moscow, Russia

¹ National Institute for Fusion Science, Toki, Japan

² École Polytechnique Fédérale de Lausanne (EPFL), Centre de Recherches en Physique des Plasmas, Association Euratom-Confédération Suisse, CH-1015 Lausanne, Switzerland

³ Max-Planck-Institute für Plasmaphysik, Garching, FRG, Germany

⁴ Max-Planck-Institute für Plasmaphysik, Greifswald, FRG, Germany

E-mail: isaev@nfi.kiae.ru

Received 18 December 2008, accepted for publication 27 April 2009

Published 4 June 2009

Online at stacks.iop.org/NF/49/075013

Abstract

Total bootstrap current calculations with the updated VENUS+ δf code that incorporates energy convolution and the momentum correction technique have been performed for the reference tokamak JT-60U cases and for the experimental Large Helical Device (LHD, NIFS, Japan) configurations with different magnetic axis positions. The VENUS+ δf results have been compared with the corresponding tokamak results of the neoclassical bootstrap current models for the general axisymmetric equilibria and arbitrary collisionality regime, as well as with the corresponding 3D SPBSC code numerical predictions and with the LHD experimental tendency.

PACS numbers: 52.25.Fi, 52.55.Hc, 52.65.Pp

(Some figures in this article are in colour only in the electronic version)

1. Introduction

Neoclassical theory in tokamaks is believed to be partially validated by the examination of the transport properties parallel to the magnetic field lines. Complete and accurate bootstrap current formulae have been obtained for general axisymmetric equilibria and arbitrary collisionality in [1, 2]. Very good quantitative agreement has been found between parallel electric field evolution expected from these formulae and that measured in the DIII-D tokamak [3].

Validation of the bootstrap current models in non-axisymmetric stellarator/heliotron configurations has been performed for the Wendelstein-7AS (Germany) device [4] with the drift-kinetic equation solver (DKES) code [5] and for the Large Helical Device (LHD, Japan) [6] with the SPBSC code [7], based on the connection formulae between different collisional regimes. However, large DKES error bars in the long-mean-free-path regime and the difference between the monoenergetic bootstrap current coefficients, calculated with the DKES and SPBSC codes for some 3D configurations [8], required further calculations with other bootstrap current

models and codes. Experimental verification of the validity of some of the earlier bootstrap current models in 3D systems was examined in [9].

Recently very good agreement [10, 11] of the monoenergetic particle bootstrap current coefficients for three various stellarator configurations (LHD, NCSX, W7X) was obtained by quite different codes (DKES, VENUS+ δf [12], NEO-MC [13] and NEO-2 [14]). Additional numerical efforts have been devoted with the VENUS+ δf code to simulate the effect of different magnetic axis positions on the monoenergetic bootstrap current coefficients in LHD [15]. Good qualitative agreement of the VENUS+ δf code results with the LHD experimental results and with the SPBSC predictions has been obtained provided that significant simplifying assumptions are invoked. The bootstrap current is characterized by the relative amplitude and by the sign for a given toroidal configuration. However, our previous work [15] included only a monoenergetic ensemble of particles and only pitch-angle scattering in the collision operator, which is insufficient to evaluate the bootstrap current quantitatively.

In this paper we present the updated VENUS+ δf code results for the total bootstrap current which include the Maxwellian energy distribution of particles, momentum correction terms, temperature and plasma density gradients. Section 2 describes the reference axisymmetric JT-60U tokamak [16] ion bootstrap current in different collisionality regimes on different plasma surfaces, calculated with the 3D VENUS+ δf code and with the Fokker–Planck tokamak solver CQLP [1, 2] with the full collision operator. In section 3 the updated VENUS+ δf code is applied to 3D LHD configurations with different magnetic axis positions aimed at comparing the VENUS+ δf and SPBSC numerical predictions with the experimental LHD bootstrap current.

2. Reference case: JT-60U tokamak ion bootstrap current density

In this section we perform the comparison of the bootstrap current density in the JT-60U tokamak with minor and major radii 1.0 m and 3.0 m, respectively, calculated with the CQLP code and with the updated VENUS+ δf code.

The reference code CQLP [1, 2] solves the linearized Fokker–Planck equation on a magnetic flux surface with a label s , proportional to the square of the normalized minor radius ($s = 1.0$ correspond to the plasma boundary), using the exact axisymmetric magnetic configuration and the full collisional operator. For the ion bootstrap current density j_{\parallel} in the plasma with temperature $T(s)$ and plasma density $n(s)$, the CQLP code computations are based on the expression

$$\langle j_{\parallel} B \rangle = -I(s)L_{31} \left(T \frac{dn}{ds} + (1 + \alpha)n \frac{dT}{ds} \right), \quad (1)$$

where B is the magnetic field strength, $I(s)$ is the poloidal current flux function, the coefficients L_{31} and α have strong dependence on trapped particle fraction and collisionality (see equations (12)–(17) in [1, 2]). This neoclassical bootstrap current model has been successfully tested in the DIII-D tokamak [3] and has also been applied to analyze neoclassical tearing modes.

Monte Carlo simulations with a time varying weighting (δf) scheme for neoclassical transport have been successfully used in several codes in tokamak geometry [17–22]. Additional efforts have been devoted to achieve energy and momentum conservation with the help of different correction terms [18, 23, 24]. To calculate neoclassical transport in heliostars/stellarators, the VENUS+ δf code uses accurate VENUS guiding centre numerical orbits [25] in Boozer coordinates [26] calculated with the ideal 3D MHD code TERPSICHORE [27]. The Coulomb collisions with the velocity dependent collision frequency $\nu(v)$ are implemented in two steps. Pitch-angle scattering is modelled by a standard Monte Carlo procedure [28], and then the parallel momentum P_{\parallel} conservation in the updated VENUS+ δf code is achieved by the marker(particle) weight δf correction term [21]

$$\Delta \delta f = \frac{-v v_{\parallel} \Delta P_{\parallel} f_M}{\sum v v_{\parallel}^2 f_M d\Omega}, \quad (2)$$

where the change in the momentum in the Monte Carlo step $\Delta P_{\parallel} = \sum \delta v_{\parallel} \delta f d\Omega$, v_{\parallel} is a particle velocity component parallel to the magnetic field, $d\Omega$ is the phase-space volume

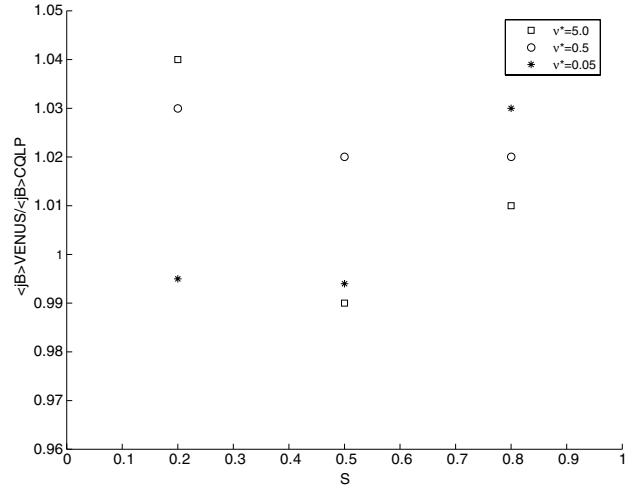


Figure 1. The ratio between the bootstrap current densities calculated with the VENUS+ δf code and the CQLP code for the JT-60U tokamak. Results with constant temperature profile ($dn/ds = -1$, $dT/ds = 0$) are shown for normalized collisional frequencies $\nu^* = 5.0$ (squares), $\nu^* = 0.5$ (circles), $\nu^* = 0.05$ (stars) for flux labels $s = 0.2, 0.5, 0.8$.

of the particle with energy E and mass m , $f_M(s, E) = n(s)(2\pi T(s)/m)^{-3/2} e^{-E/T(s)}$ is a local Maxwellian on the flux surface. A detailed description of three-dimensional VENUS+ δf bootstrap current calculation module is provided in [12].

In the VENUS+ δf code, the ion bootstrap current density with a particle charge q_i and density n is computed from time-averaging equation

$$\langle j_{\parallel} B \rangle = \left\langle n q_i \frac{\sum v_{\parallel} B \delta f d\Omega}{\sum f_M d\Omega} \right\rangle, \quad (3)$$

in the case of the equal impact of ions and electrons to the total bootstrap current, the flux derivative of the total current dJ_{BS}/ds is obtained from equation

$$J'_{\text{BS}}(s) = 2\pi a^2 \langle j_{\parallel} B \rangle / B_0, \quad (4)$$

where a is the average minor plasma radius, the total bootstrap current is

$$J_{\text{BS}} = \int_0^1 J'_{\text{BS}}(s) ds. \quad (5)$$

Figure 1 presents the ratio between the bootstrap current density calculated with the VENUS+ δf code (3) and with the CQLP code using formula (1) for flat temperature profile (only ion density gradient effects) on different plasma flux surfaces $s = 0.2, 0.5, 0.8$ and for several collisionality regimes $\nu^* = 0.05, 0.5, 5.0$. This ratio is equal to unity within the accuracy of Monte Carlo method, which is inversely proportional to the number of particles. In this figure, a deviation between the two codes of less than 5% is achieved with the ensemble composed of 8–40 monoenergetic groups with energies distributed in accordance with the Maxwellian law. Each monoenergetic group consists of 50–1000 markers uniformly distributed with respect to the pitch angle variable. A steady-state solution of the bootstrap current is obtained after several collision steps, after that the parallel momentum is conserved with an accuracy of 5–20%. From figure 1, one can conclude that

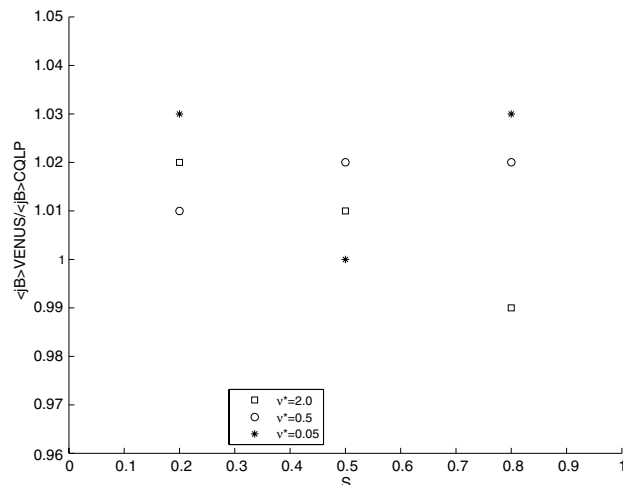


Figure 2. The ratio between the bootstrap current densities calculated with the VENUS+ δf code and the CQLP code for the JT-60U tokamak. Results with constant density profile ($dn/ds = 0$, $dT/ds = -1$) are shown for normalized collisional frequencies $\nu^* = 2.0$ (squares), $\nu^* = 0.5$ (circles), $\nu^* = 0.05$ (stars) for flux labels $s = 0.2, 0.5, 0.8$.

the VENUS+ δf code reproduces well the main collisional dependence of the CQLP bootstrap current coefficient L_{31} in tokamaks for different plasma radii. Energy slowing down has a small effect on the VENUS+ δf solution during several collisional times. Plasma edge and magnetic axis regions as well as wide-orbit effects are not considered in this comparison. Since the VENUS+ δf uses 3D VMEC equilibrium inputs with poor force balance in the regions near the magnetic axis and near the boundary [29], these regions are excluded in this paper. In this work, we take into account only thin orbits and neglect wide orbit effects.

Good agreement of the 3D VENUS+ δf code with CQLP bootstrap current density for the flat density profile and the linear $1 - s$ temperature profile (that serves to quantify the effect of the bootstrap current coefficient α of equation (2)) is shown in figure 2. The ratio of the ion bootstrap current densities, calculated with the two codes, is equal to unity within an accuracy of 5% for different magnetic surfaces $s = 0.2, 0.5, 0.8$ for normalized collisional frequencies $\nu^* = 0.05, 0.5, 2.0$.

The CPU runtime on Pentium 4-type processors with the VENUS+ δf code is equal to several minutes for these cases. The good agreement obtained with the known CQLP code results in these reference tokamak calculations with the density and temperature gradient driving terms, in addition to the momentum conservation technique, provides us the basis and credibility to perform the total bootstrap current calculations for more complicated heliotron/stellarator configurations of the LHD in the next section with the VENUS+ δf code.

3. The bootstrap current calculations in the LHD with the SPBSC and the VENUS+ δf codes

The LHD is a superconducting Large Helical Device with a helical field and with poloidal winding number $l = 2$ and $m = 10$ toroidal field periods [30]. From experimental measurements of the non-inductive current, the dependence

of the bootstrap current on the β value and the magnetic axis locations were studied and compared with the theoretical expectations by the SPBSC code [6]. The electron temperature on the axis was $T_{e0} = 1-2$ keV, the electron density $n_{e0} = 1-3 \times 10^{19} \text{ m}^{-3}$, these parameters correspond to the normalized collisional frequency $0.1 < \nu^* < 10$; the β values lay in the range 0.33–0.41%. The maximal positive bootstrap current of 25 kA was experimentally obtained for the configuration with a magnetic axis position $R_{ax} = 3.90$ m. An outward shift of the magnetic axis leads to a decrease in the toroidal current. According to SPBSC predictions, the configuration with $R_{ax} = 4.05$ m can have a negative bootstrap current of -5 kA, however, the experimental measurements yield between -2 and $+2$ kA (depending on the different temperature and density values).

In order to approach these LHD experimental results and the SPBSC quasi-analytical fluid moment approach [7], the dimensionless bootstrap current coefficient, normalized to the collisionless tokamak asymptote, has been calculated recently with the VENUS+ δf code [15]. The main experimental dependence of the bootstrap current coefficient with respect to the magnetic axis outward shift has been reproduced both with the SPBSC and VENUS+ δf codes.

In this paper we present the LHD total bootstrap current flux derivative dJ_{BS}/ds calculations with both SPBSC and VENUS+ δf codes with different plasma density profiles for the LHD configurations with different magnetic axis positions. A linear temperature dependence on the flux surface label $T = T_0(1 - s)$ is prescribed. The updated VENUS+ δf code includes the momentum correction term (2) and a Maxwellian distribution of the energies. Ion and electron density and temperature profiles are taken as equal, while the radial electric field and island effects are neglected. In this paper, we select the magnetic field on axis $B_0 = 3.0$ T and the effective plasma charge Z_{eff} equals to unity.

The bootstrap current flux derivatives dJ_{BS}/ds as a function of flux label s for the magnetic axis position of $R_{ax} = 3.75$ m are presented in figure 3(a) for the linear $n = n_0(1 - s)$ and in figure 3(b) for the flattened $n = n_0(1 - s^4)$ plasma density profiles. Given central values of the temperature $T_0 = 1.0$ keV and the density $n_0 = 10^{19} \text{ m}^{-3}$, the normalized collisional frequency corresponds to $\nu^* = 0.13$ on the flux label $s = 0.5$. The SPBSC code results are shown as circles and crosses. The integration of the dJ_{BS}/ds function gives the total bootstrap currents J_{BS} of 5.24 kA and 6.45 kA for the linear and flattened current density profiles, respectively.

The VENUS+ δf code, with 20 000 particles on each of 16 processors, distributed in energy according to the Maxwellian law, demonstrated after several collisional times steady state bootstrap current solutions with Monte Carlo error bars of 10–15% (shown as squares in figures 3(a) and diamonds in 3(b)). The triangles in figure 3(a) show the results without the momentum conservation.

The total bootstrap current $J_{BS} \approx 7-9$ kA, calculated with the VENUS+ δf code, is about 20–40% larger than that obtained with the SPBSC code. This difference is connected with the different simulation models included in these different codes. In the transitional regime between the plateau and collisionless limits, the bootstrap current coefficients of monoenergetic particles, calculated with the

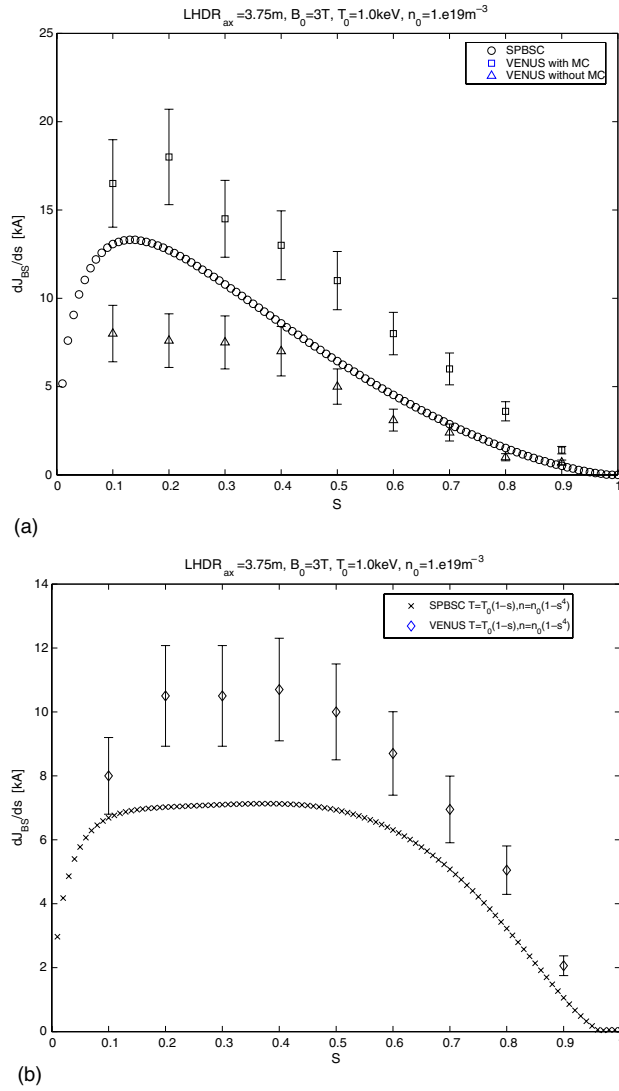


Figure 3. (a) The LHD $R_{ax} = 3.75$ m bootstrap current derivative dJ_{BS}/ds versus the flux label s with the linear plasma density profile $n = n_0(1-s)$, $n_0 = 10^{19} \text{ m}^{-3}$, $T_0 = 1.0$ keV calculated with the SPBSC code (circles) and with the VENUS+ δf code (squares with momentum conservation, triangles without momentum conservation). (b) The LHD $R_{ax} = 3.75$ m bootstrap current derivative dJ_{BS}/ds versus the flux label s with the flattened plasma density profile $n = n_0(1-s^4)$, $n_0 = 10^{19} \text{ m}^{-3}$, $T_0 = 1.0$ keV calculated with the SPBSC code (crosses) and with the VENUS+ δf code (diamonds).

DKES, NEO, VENUS+ δf codes, significantly exceed the asymptotical analytical collisionless limit [10]. In contrast, the SPBSC code is based on the monotonic approximation between the semi-analytical limits and achieves its maximum value in the collisionless limit.

The accuracy of the VENUS+ δf code calculations can be improved by increasing the number of particles and, correspondingly, by increasing the required CPU time.

For the complicated 3D structure of the LHD magnetic field spectrum (up to 400 Boozer [26] poloidal and toroidal modes), the accurate fourth order Runge–Kutta integration of drift orbits in the VENUS+ δf code has been applied. For a given collisional regime, one VENUS+ δf code run for one selected LHD magnetic surface requires about 20 CPU

hours on each processor. One bootstrap current profile with 10 radial points requires 200 h of CPU time on a 16-node Pentium 4-type 3.2 GHz scalar cluster; the total CPU time required for this bootstrap current calculations is equal to 3200 h. For comparison purposes, the SPBSC code is able to calculate the bootstrap current profile with 100 radial points during just 1 min on one NEC-SX8 vector processor.

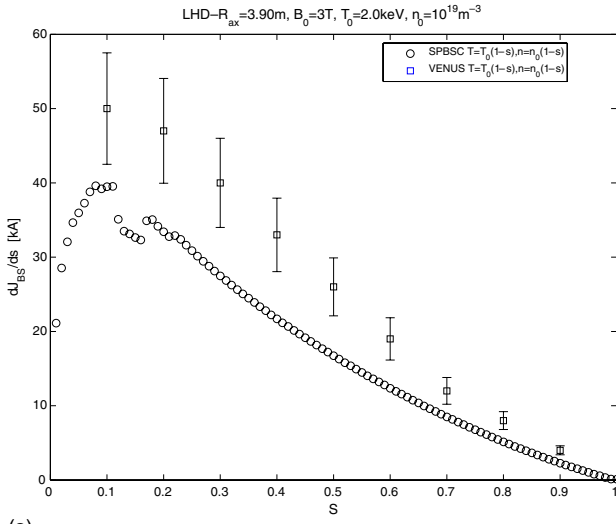
The experimentally measured total bootstrap current in the LHD $R_{ax} = 3.75$ m configuration with the $T_0 = 1.0$ keV, $n_0 = 10^{19} \text{ m}^{-3}$, $B_0 = 1.5$ T and $Z_{eff} = 2.0$ is equal to 20–30 kA, which corresponds to the SPBSC and the VENUS+ δf predictions within a factor of 2–3. Accurate comparison with the LHD experimental results will be performed in the near future with the experimentally obtained density and temperature profiles for ions and electrons.

Figures 4(a) and (b) show the bootstrap current derivative dJ_{BS}/ds profiles for the LHD $R_{ax} = 3.90$ m configuration, calculated with linear $n = n_0(1-s)$ and flattened $n = n_0(1-s^4)$ density profiles. Central values of the density $n_0 = 10^{19} \text{ m}^{-3}$ and the temperature $T_0 = 2.0$ keV are used for this case that corresponds to a normalized collisional frequency of $\nu^* = 0.06$ on the flux label $s = 0.5$. The integration of the dJ_{BS}/ds function, obtained with the SPBSC code, yields total bootstrap currents J_{BS} of 17.8 (circles) kA and 13.3 (crosses) kA for the linear and flattened density profiles, respectively. For this LHD $R_{ax} = 3.90$ m configuration, the linear plasma density significantly increases the total bootstrap current. One can also see the resonant effects (jumps and spike) between $s = 0.1$ and $s = 0.2$ magnetic surfaces on the SPBSC bootstrap current profiles.

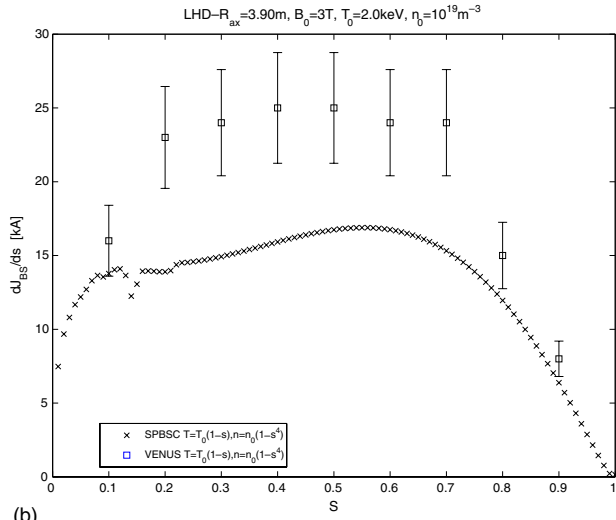
The VENUS+ δf code results with the resonance detuning are shown as squares with error bars of 10–15% for the linear (figure 4(a)) and for the flattened (figure 4(b)) plasma densities. The total bootstrap currents $J_{BS} \approx 24$ kA (figure 4(a)) and $J_{BS} \approx 18$ kA (figure 4(b)), calculated with the VENUS+ δf code, are 20–40% larger than the currents obtained with the SPBSC code. This difference is related to the different simulation models included in the SPBSC and the VENUS+ δf codes and should be visible in the low collisionality regime.

The experimentally measured total bootstrap current in the LHD $R_{ax} = 3.90$ m configuration with $T_0 = 2.0$ keV, $n_0 = 10^{19} \text{ m}^{-3}$, $B_0 = 1.5$ T and $Z_{eff} = 2.0$ is equal to 15–30 kA, which corresponds to the SPBSC and the VENUS+ δf predictions within a factor of 1–2.

The simulated bootstrap current derivatives dJ_{BS}/ds for the LHD $R_{ax} = 4.00$ m configuration are shown in figure 5(a) with the linear plasma density profile and in figure 5(b) with the flattened plasma density profile. The SPBSC code results with central plasma density and temperature, $n_0 = 0.5 \times 10^{19} \text{ m}^{-3}$, and $T_0 = 1$ keV are shown by circles (figure 5(a)) and crosses (figure 5(b)), respectively. The normalized collision frequency ν^* on the magnetic surface $s = 0.5$ is equal to 0.05. Several resonance effects are visible on the SPBSC curves—near the $s = 0.14$, $s = 0.6$ and $s = 0.83$ magnetic surfaces. The VENUS+ δf code uses the Boozer magnetic field spectrum, obtained from the TERPSICHORE code with the resonance detuning. This resonance detuning provides a smooth behaviour of flux functions around the resonance surfaces. The SPBSC code without resonance detuning shows abrupt discontinuous changes in the bootstrap current profile near the resonances [31].



(a)



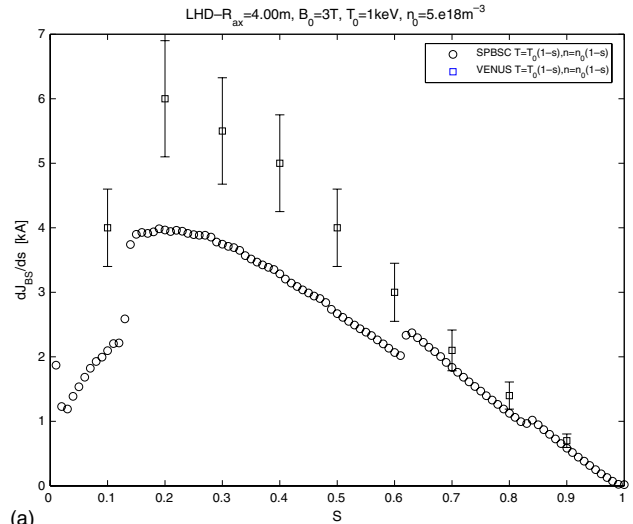
(b)

Figure 4. (a) The LHD $R_{ax} = 3.90$ m bootstrap current derivative dJ_{BS}/ds versus the flux label s with the linear plasma density profile $n = n_0(1 - s)$, $n_0 = 10^{19} \text{ m}^{-3}$, $T_0 = 2.0 \text{ keV}$ calculated with the SPBSC code (circles) and with the VENUS+ δf code (squares). (b) The LHD $R_{ax} = 3.90$ m bootstrap current derivative dJ_{BS}/ds versus the flux label s with the flattened plasma density profile $n = n_0(1 - s^4)$, $n_0 = 10^{19} \text{ m}^{-3}$, $T_0 = 2.0 \text{ keV}$ calculated with the SPBSC code (crosses) and with the VENUS+ δf code (squares).

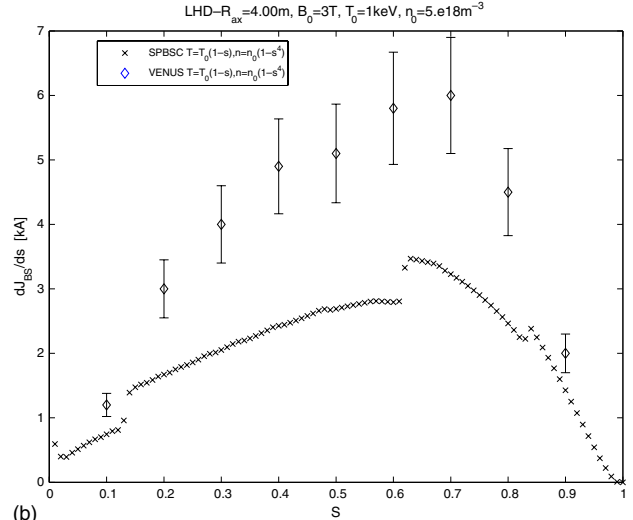
The total bootstrap currents J_{BS} , calculated with the VENUS+ δf code (marked as squares in figure 5(a) and diamonds in figure 5(b)) with error bars of 10–15%, are approximately equal to 3.2 kA (figure 5(a)) and 3.7 kA (figure 5(b)), which is 1–2 kA larger than the SPBSC code results.

The total bootstrap currents in the LHD configuration with the magnetic axis position of $R_{ax} = 4.00$ m, calculated with the SPBSC code for $n_0 = 0.5 \times 10^{19} \text{ m}^{-3}$ and $T_0 = 1.0 \text{ keV}$, are equal to 2.24 kA and 2.01 kA for the linear and for the flattened plasma density profiles, respectively. This value corresponds within a factor of 2 to the experimentally measured bootstrap current of 4 kA (for $B_0 = 1.5 \text{ T}$ and $Z_{eff} = 2.0$).

Following the previous style, figures 6(a) and (b) show the bootstrap current derivative dJ_{BS}/ds profiles for the LHD



(a)



(b)

Figure 5. (a) The LHD $R_{ax} = 4.00$ m bootstrap current derivative dJ_{BS}/ds versus the flux label s with the linear plasma density profile $n = n_0(1 - s)$, $n_0 = 0.5 \times 10^{19} \text{ m}^{-3}$, $T_0 = 1.0 \text{ keV}$ calculated with the SPBSC code (circles) and with the VENUS+ δf code (squares). (b) The LHD $R_{ax} = 4.00$ m bootstrap current derivative dJ_{BS}/ds versus the flux label s with the flattened plasma density profile $n = n_0(1 - s^4)$, $n_0 = 0.5 \times 10^{19} \text{ m}^{-3}$, $T_0 = 1.0 \text{ keV}$ calculated with the SPBSC code (crosses) and with the VENUS+ δf code (diamonds).

$R_{ax} = 4.05$ m configuration using linear (figure 6(a)) $n = n_0(1 - s)$ and flattened (figure 6(b)) $n = n_0(1 - s^4)$ density profiles, respectively. Central values of the density $n_0 = 2.0 \times 10^{19} \text{ m}^{-3}$ and the temperature $T_0 = 0.5 \text{ keV}$ are used for this case, corresponding to a normalized collisional frequency of $\nu^* = 2.0$ on the flux label $s = 0.64$. The integration of the dJ_{BS}/ds functions, obtained with the SPBSC code, yields small negative total bootstrap currents J_{BS} of -0.86 kA and -0.31 kA for the linear (crosses) and flattened (circles) density profiles, respectively. Several resonant effects on the SPBSC bootstrap current profiles are visible near the magnetic surfaces $s = 0.12, 0.18, 0.24, 0.35, 0.40, 0.58$. The VENUS+ δf code results with the resonance detuning are shown as squares (figure 6(a)) with error bars around 15% for the linear plasma density and as diamonds (figure 6(b)) for the

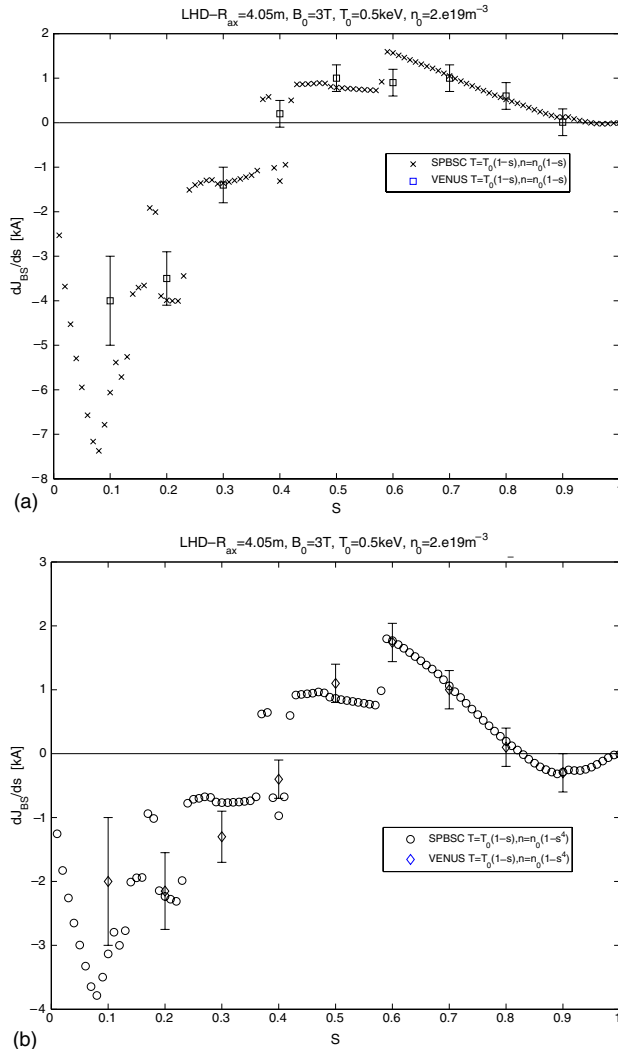


Figure 6. (a) The LHD $R_{ax} = 4.05$ m bootstrap current derivative dJ_{BS}/ds versus the flux label s with the linear plasma density profile $n = n_0(1 - s)$, $n_0 = 2.0 \times 10^{19} \text{ m}^{-3}$, $T_0 = 0.5$ keV calculated with the SPBSC code (crosses) and with the VENUS+ δf code (squares). (b) The LHD $R_{ax} = 4.05$ m bootstrap current derivative dJ_{BS}/ds versus the flux label s with the flattened plasma density profile $n = n_0(1 - s^4)$, $n_0 = 2.0 \times 10^{19} \text{ m}^{-3}$, $T_0 = 0.5$ keV calculated with the SPBSC code (circles) and with the VENUS+ δf code (diamonds).

flattened plasma density profile. For this highly collisional regime, the VENUS+ δf code results agree well with the SPBSC code results except the near axis region and the regions near the resonances.

The experimentally measured total bootstrap current in the LHD $R_{ax} = 4.05$ m configuration is very small and can be negative up to -5 kA, which corresponds to the SPBSC and the VENUS+ δf predictions within a factor of 1–2.

Figure 7 shows the normalized collisional frequency ν^* profiles, calculated with the SPBSC code, corresponding to the LHD configurations examined in figure 3(b) (shown as circles, $R_{ax} = 3.75$ m, $T_0 = 1$ keV, $n_0 = 10^{19} \text{ m}^{-3}$), in figure 4(b) (crosses, $R_{ax} = 3.90$ m, $T_0 = 2$ keV, $n_0 = 10^{19} \text{ m}^{-3}$), in figure 5(b) (squares, $R_{ax} = 4.00$ m, $T_0 = 1$ keV, $n_0 = 0.5 \times 10^{19} \text{ m}^{-3}$) and in figure 6(b) (stars, $R_{ax} = 4.05$ m, $T_0 = 0.5$ keV, $n_0 = 2.0 \times 10^{19} \text{ m}^{-3}$), respectively. For all the

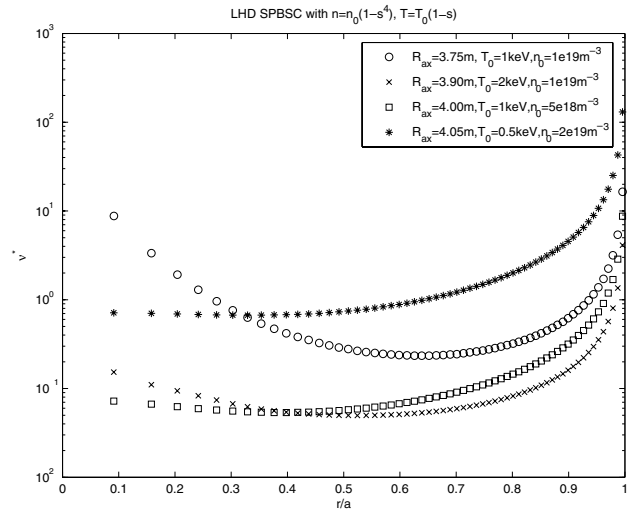


Figure 7. The normalized collisional frequency ν^* versus the normalized plasma radius $r/a = s^{0.5}$, calculated with the SPBSC code, corresponding to the LHD configurations explored in figure 3(b) (shown as circles, $R_{ax} = 3.75$ m, $T_0 = 1$ keV, $n_0 = 10^{19} \text{ m}^{-3}$), in figure 4(b) (crosses, $R_{ax} = 3.90$ m, $T_0 = 2$ keV, $n_0 = 10^{19} \text{ m}^{-3}$), in figure 5(b) (squares, $R_{ax} = 4.00$ m, $T_0 = 1$ keV, $n_0 = 0.5 \times 10^{19} \text{ m}^{-3}$) and in figure 6(b) (stars, $R_{ax} = 4.05$ m, $T_0 = 0.5$ keV, $n_0 = 2.0 \times 10^{19} \text{ m}^{-3}$).

cases considered, the normalized collisional frequency ν^* is enclosed in the interval [0.05–10]. Within these collisionality regimes, a reasonable discrepancy of 20–50% between the SPBSC and the VENUS+ δf code predictions, obtained in our calculations, is connected with the different simulation models which are used in these codes.

As was reported in [8], an even larger difference of the order of 2–4 times, between the bootstrap current coefficients predicted by the Shaing–Callen model and the monoenergetic bootstrap current coefficients calculated with the DKES, NEO, VENUS+ δf codes can be observed for the LHD configurations in the long-mean-free-path regimes ($\nu^* < 0.01$). The momentum conservation increases the bootstrap current results obtained with the VENUS+ δf code by a factor ~ 2 for the LHD configurations examined here (triangles in figure 3(a) show the results without the momentum conservation).

4. Summary

The updated VENUS+ δf code with the momentum correction term and Maxwellian distribution of particles has been successfully applied for the calculations of the bootstrap current in the JT-60U reference tokamak cases and for 3D LHD configurations.

The essential contribution in the 3D VENUS+ δf code development includes the transition from monoenergetic to Maxwellian distribution of particles; an ion momentum conservation procedure in the collision operator for like-particles; plasma temperature and density gradient effects. This contribution provides the next step towards an accurate calculation of the bootstrap current profile in non-axisymmetric magnetic configurations. In this work, we calculate with the VENUS+ δf code only the ion bootstrap current. The total bootstrap current is obtained using the

assumption of the equal impact of ions and electrons. This assumption helps us to compare the VENUS+ δf code results with the results obtained from the reference tokamak CQLP code [1, 2] and the non-axisymmetric SPBSC code. In the near future, we plan to calculate the electron bootstrap current separately using the simulation model developed in [22, 32, 33]. Consistent radial electric fields will also be considered later using the ambipolarity condition as in [34].

Good agreement that tested the density and temperature gradients bootstrap current driving terms has been obtained with the tokamak reference code CQLP with the full collisional operator. Energy slowing down in the collision operator has not been included so far in the VENUS+ δf code. A more detailed investigation of this problem will be considered in the near future.

In this work, the VENUS+ δf code has been applied for the first time to calculate the total bootstrap current in a range of LHD configurations. Previously, large computational work for this task has been performed with the SPBSC code based on the Shaing–Callen approach and the semi-analytical fit between the different collisionality regimes. For highly collisional regimes (the normalized collisional frequency $\nu^* > 1$), the different simulation codes give very good agreement for the monoenergetic bootstrap current calculations [11]. The total bootstrap current calculations, performed with the SPBSC and with the VENUS+ δf codes for the LHD- $R_{ax} = 4.05$ m configuration in the highly collisional regimes, also demonstrate quite satisfactory agreement for the LHD configurations.

The main experimental effect of the outward shifted magnetic axis on the bootstrap current has been confirmed in the simulations. For the LHD configurations with the magnetic axis positions of $R_{ax} = 3.75$ m and $R_{ax} = 3.90$ m the calculated bootstrap current J_{BS} lies in the limits 15–30 kA, while for $R_{ax} = 4.00$ m we get $J_{BS} \approx 5$ kA and for $R_{ax} = 4.05$ m the bootstrap current is small and can be negative up to -5 kA. Calculations have been performed with linear temperature and density profiles. In addition a flattened density profile has been used to approach the experimentally measured results. We assumed that both ions and electrons have the same temperature and density profiles, while radial electric fields and islands were neglected.

The difference between the SPBSC and the VENUS+ δf codes has been observed near the resonances, since the VENUS+ δf code uses the magnetic spectrum from the TERPSICHORE code with resonance detuning. Another difference in the results should be visible for the low collisionality regime due to the different models implemented into the SPBSC and VENUS+ δf codes. Indeed a difference about 20–40% has been observed for the regions with low collisionality ($\nu^* < 1$) for cases with the magnetic axis positions $R_{ax} = 3.75$ m, 3.90 m, 4.00 m.

For the complicated magnetic field spectrum of the LHD configurations, the VENUS+ δf code requires significant CPU resources. The calculations were performed for several collisional times, the steady-state solutions were obtained with error bars on the level of 10–15%. The accuracy of these calculations can be in principle improved with the help of large cluster usage and better code performance.

In order to compare our neoclassical simulations with the LHD experimental results, we will use in the near future

experimentally obtained density and temperature profiles for ions and electrons. The LHD super dense core discharges with internal diffusion barriers [35] should also be investigated in the future with new tools, because at the moment only the ideal nested surfaces without magnetic islands are considered in our 3D bootstrap codes.

Acknowledgments

The authors thank S.P. Hirshman for providing us the VMEC code. The work was supported in part by NIFS/NINS under the Project of Formation of International Network of Scientific Collaboration (Japan), by the Fond National Suisse pour la Recherche Scientific and by Euratom.

The computational results were performed on the Pleiades2 cluster (EPFL, Switzerland) and on the NEC-SX8 and Optron cluster (NIFS, Japan).

Euratom © 2009.

References

- [1] Sauter O., Angioni C. and Lin-Liu Y.R. 1999 *Phys. Plasmas* **6** 2834
- [2] Sauter O., Angioni C. and Lin-Liu Y.R. 2002 *Phys. Plasmas* **9** 5140 (erratum)
- [3] Wade M.R., Murakami M. and Politzer P.A. 2004 *Phys. Rev. Lett.* **92** 235005
- [4] Maaßberg H. *et al* 2005 *Plasma Phys. Control. Fusion* **47** 1137
- [5] van Rij W.I. and Hirshman S.P. 1989 *Phys. Fluids B* **1** 563
- [6] Watanabe K.Y. *et al* 2002 *J. Plasma Fusion Res. Ser.* **5** 124
- [7] Watanabe K.Y. *et al* 1992 *Nucl. Fusion* **44** 1499
- [8] Beidler C.D. *et al* 2003 Neoclassical transport in stellarators—results from an international collaboration *Proc. 30th EPS Conf. on Controlled Fusion and Plasma Physics (St Petersburg, Russia, 2003)* (ECA) vol 27A P-3.2 http://epsppd.epfl.ch/StPetersburg/PDF/P3_002.PDF
- [9] Murakami M. *et al* 1991 *Phys. Rev. Lett.* **66** 707
- [10] Allmaier K. *et al* 2007 *Proc. Joint Conf. 17th Int. Toki Conf. and 16th Int. Stellarator/Heliotron Workshop (Toki, Japan, 15–19 October 2007)* p 615
- [11] Beidler C.D. *et al* 2008 *Proc. 22nd Int. Conf. on Fusion Energy (Geneva, Switzerland, 2008)* (Vienna: IAEA) CD-ROM file TH/P8-10 and <http://www.naweb.iaea.org/napc/physics/FEC/FEC2008/html/index.htm>
- [12] Isaev M.Yu. *et al* 2006 *Fus. Sci. Technol.* **50** 440
- [13] Allmaier K. *et al* 2008 *Phys. Plasmas* **15** 072512
- [14] Kernbichler W. *et al* 2005 Calculation of neoclassical transport in stellarators with finite collisionality using integration along magnetic field lines *Proc. 32nd EPS Conf. on Plasma Physics (Tarragona, Spain, 2005)* P1-111 http://epsppd.epfl.ch/Tarragona/PDF/P1_111.PDF
- [15] Isaev M.Yu. *et al* 2008 *Plasma Fusion Res.* **3** 036
- [16] Kikuchi M. *et al* 1990 *Nucl. Fusion* **30** 343
- [17] Xu X.Q. and Rosenbluth M.N. 1991 *Phys. Fluids B* **3** 627
- [18] Lin Z., Tang W.M. and Lee W.W. 1995 *Phys. Plasmas* **2** 2975
- [19] Sasinowski M. and Boozer A.H. 1995 *Phys. Plasmas* **2** 610
- [20] Brunner S., Valeo E. and Krommes J.A. 2000 *Phys. Plasmas* **7** 2810
- [21] Bergmann A., Peeters A.G. and Pinches S.D. 2001 *Phys. Plasmas* **8** 5192
- [22] Wang W.X. *et al* 2006 *Phys. Plasmas* **13** 082501
- [23] Wang W.X. *et al* 1999 *Plasma Phys. Control. Fusion* **41** 1091
- [24] Satake S., Sugama H. and Watanabe T.-H. 2007 *Nucl. Fusion* **47** 1258
- [25] Fischer O. *et al* 2002 *Nucl. Fusion* **42** 817

- [26] Boozer A.H. 1980 *Phys. Fluids* **23** 904
- [27] Anderson D.V. *et al* 1990 *J. Supercomput. Appl.* **4** 34
- [28] Boozer A.H. and Kuo-Petravic G. 1981 *Phys. Fluids* **24** 851
- [29] Sanchez R. *et al* 2001 *Comput. Phys. Commun.* **141** 55
- [30] Motojima O. *et al* 2003 *Nucl. Fusion* **43** 1674
- [31] Isaev M.Yu. *et al* 2003 SPBSC-TERPSICHORE bootstrap current benchmark for the low collisionality regime *Proc. 30th EPS Conf. on Controlled Fusion and Plasma Phys.* (St Petersburg, Russia, 2003) (ECA) vol 27A, P-4.9 http://epsppd.epfl.ch/StPetersburg/PDF/P4_009.PDF
- [32] Bergmann A., Strumberger E. and Peeters A.G. 2005 *Nucl. Fusion* **45** 1255
- [33] Wang W.X. *et al* 2004 *Comput. Phys. Commun.* **164** 178
- [34] Yokoyama M. *et al* 2005 *Fus. Sci. Technol.* **50** 327
- [35] Ohyaibu N. *et al* 2006 *Plasma Phys. Control. Fusion* **48** B383